

Reflections on a Measurement of the Gravitational Constant Using a Beam Balance and 13 Tons of Mercury

S. Schlamminger¹, R.E. Pixley², F. Nolting³, J. Schurr⁴ and U. Straumann²

¹National Institute of Standards and Technology, Gaithersburg, MD, USA.

²Physik-Institut der Universität Zürich, Zürich, Switzerland.

³Paul Scherrer Institut, Villigen, Switzerland.

⁴Physikalisch Technische Bundesanstalt, Braunschweig, Germany.

October 15, 2018

Abstract

In 2006, a final result of a measurement of the gravitational constant G performed by researchers at the University of Zürich was published. A value of $G = 6.674\,252(122) \times 10^{-11} \text{ m}^3 \text{ kg}^{-1} \text{ s}^{-2}$ was obtained after an experimental effort that lasted over one decade. Here, we briefly summarize the measurement and discuss the strengths and weaknesses of this approach.

1 Introduction

The existence of the Zürich G experiment is due to an article published in 1986 by Fischbach et al. [1] analyzing old data taken by von Eötvös [2] to test the universality of free fall. A deviation was found in the intermediate-range (about 200 m) coupling, giving rise to the so-called fifth force. The existence of such a fifth force at the strength conjectured in [1] was quickly found to be in error [3]. However, Fischbach's article started a renaissance of gravity experiments at universities world wide. Walter Kündig at the University of Zürich started an experiment aimed at measuring the gravitational attraction between water in a storage lake (Gigerwald lake) and two masses suspended from a balance [4]. The experiment was conducted in two different configurations. First, the test masses were vertically separated by 63 m, later by 104 m. The magnitude of the gravitational attraction was measured as the water level varied seasonally over the course of several years. As a result of the experiment, two measurements of G for an interaction range of 88 m and 112 m were obtained with relative standard-uncertainties of 1×10^{-3} and 7×10^{-4} , respectively [5]. The results were consistent with each other and consistent with the value of G from laboratory determinations. Even today, 20 years after this experiment, its results place the most stringent limit on a possible violation of the inverse square law at distances ranging from 10 m to 100 m. The largest contribution to the uncertainty of each result came from the ambiguous mass distribution of the lake. It was unclear how far the lake water penetrated the shore composed mostly of scree. It was immediately recognized that one could use the same method for a precise determination of the gravitational constant if only one had a better defined lake.

From this line of thinking, the concept of measuring G in the laboratory was conceived and the design of the experiment started in 1994. Conceptually the experiment is similar to the Gigerwald experiment with one difference: the "lake" was confined to two well characterized stainless-steel vessels each holding 500 L of liquid. In a first experiment, water was used; later, the water was replaced with mercury yielding a much larger signal.

The Zürich big G experiment ended officially in 2006, when a final report [6] on the experiment was published. The relevant details of the experiment have been summarized in the final report, two theses [7, 8] and several shorter reports [9, 10, 11, 12, 13, 14].

2 The experiment's principle

The principle of the experiment is shown in figure 1. A gravitational field is generated by two large cylinders labeled field masses (FMs). The gravitational field can be modulated by moving the FMs. During measurement,

the FMs are in either one of two positions, labeled T for together and A for apart. Two test masses (TMs) are used to probe the gravitational field. The two test masses are alternately, but never concurrently, connected to a mass comparator (balance) at the top of the experiment each by a set of two wires and a mass exchanger. While the mass comparator is calibrated in units of kg, it is used as an instrument to measure vertical force with high accuracy. The balance is calibrated by adding calibration masses to the mass pan. The reading of the balance can be converted into a force by multiplying with the value of the local acceleration, $g = 9.807\,233\,5(6)\text{ m/s}^2$ which was measured at the site.

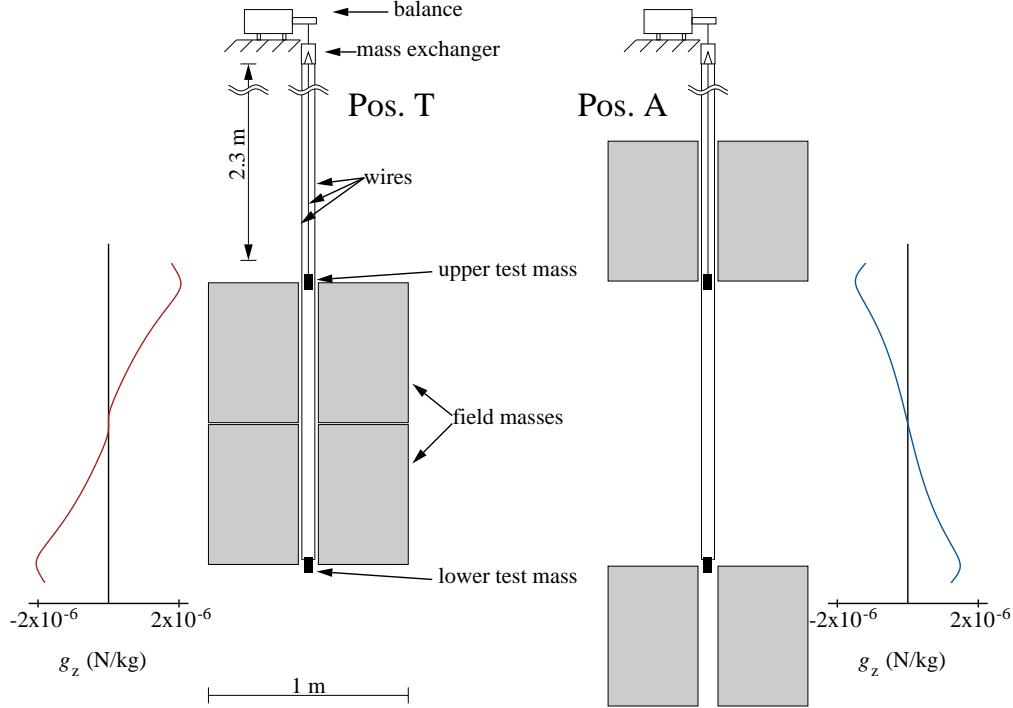


Figure 1: Principle of the Zürich G experiment. Either of the two test masses is suspended from the balance. The field masses are either in the position T (together) or A (apart) as shown on the left and right side of the figure respectively. The graphs to the side of the field masses show the vertical part of the gravitational field generated by the field masses along the symmetry axis in the center of the hollow cylinders. A downward force corresponds to a positive sign.

In the together/apart state, the difference in the force on the upper and lower test mass are given by

$$\Delta F_T = m_u g(z_u) + F_z(T, u) - m_l g(z_l) - F_z(T, l) \quad (1)$$

$$\Delta F_A = m_u g(z_u) + F_z(A, u) - m_l g(z_l) - F_z(A, l), \quad (2)$$

where $F_z(A/T, u/l)$ denotes the vertical gravitational force between the complete field mass assembly in the A/T position and the upper/lower test mass. The difference, $\Delta F_T - \Delta F_A$ is the second difference or gravitational signal and is given by

$$s = \Delta F_T - \Delta F_A = F_z(T, u) - F_z(A, u) - F_z(T, l) + F_z(A, l) = G\Gamma. \quad (3)$$

It can be seen that the mass difference between the upper and lower test masses, as well as the value of local gravity and its gradient on the test masses vanish. In our convention a positive force points downward (increasing balance reading). With this convention, $F_z(T, u)$ and $F_z(A, l)$ are positive, but $F_z(T, l)$ and $F_z(A, u)$ are negative. The second difference can be written as a product of G and a mass integration constant Γ . The mass integration constant has units of kg^2/m^2 and depends solely on the mass distributions within the field masses, the test masses, and their relative positions in the two states.

The size of the gravitational signal $s/g \approx 785\ \mu\text{g}$ was determined with an accuracy of $14.3\ \text{ng}$ using a modified

commercial mass comparator (Mettler Toledo AT1006¹). Off the shelf, this type of mass comparator is used at national metrology institutes to compare 1 kg weights with each other using the substitution method. The mass comparator is essentially a sophisticated beam balance, where a large fraction of the load on the mass pan is compensated by a fixed counter mass. Only a small part of the gravitational force on the mass pan is compensated by an electromagnetic actuator consisting of a stationary permanent magnet system and a current carrying coil attached to the balance beam. The current in the coil is controlled such that the beam remains in a constant position. The coil current is precisely measured and converted into kg. This value is shown on the display and can be transferred to a computer. Typically, the dynamic range of such a comparator is 24 g around 1000 g with a resolution of 100 ng. The comparator used in the present experiment was modified in two ways: First, the mass comparator was made vacuum compatible by stripping it of all plastic parts and separating the electronics from the weighing cell. The electronics outside the vacuum vessel was connected to the balance via vacuum feed throughs. Second, the dynamic range was reduced to 4 g thereby decreasing the resolution to 16.7 ng by simply reducing the number of turns of the coil by a factor of six. Hence, for the same applied current to the coil, the force was reduced by a factor six. Since the coil current was measured with the same electronics, the mass resolution decreased by a factor six. An additional decrease to 12.5 ng was achieved by modifying software in the balance controller.

The field masses are cylindrical vessels made from stainless steel, each with an inner volume of 500 L. The lower right panel of figure 2 shows a drawing of one vessel. Each vessel was filled with 6760 kg of mercury. A liquid was used to ensure a homogeneous density and mercury was chosen due to its high density of 13.54 g/cm³. The gravitational signal produced by the liquid is proportional to its density. Therefore, the gravitational signal due to the mercury is 13.5 times larger than that of water. However, since the contribution of the stainless steel vessels needs to be taken into account, the mercury filled vessels produce only 4.1 times the signal of the water filled vessels. The vessels contribute about 60 μ g to the signal, which is about 7.6% of the signal obtained with the mercury filled vessels, but 55% of the signal obtained with water filled vessels.

The vessels were evacuated prior to filling them with mercury to avoid trapping air. The mercury was delivered in 395 flasks, each weighing about 36.5 kg (34.5 kg mercury and 2 kg due to the steel flask). Each flask was weighed before and after its content was transferred to one of the two vessels using an evacuated transfer system. This painstakingly careful work led to a relative standard uncertainty of the mercury mass of 1.8×10^{-6} and 2.2×10^{-6} for the upper and lower vessel, respectively. The mercury for this experiment was leased, i.e., after the experiment was dismantled in December 2002 the mercury was sent back to the supplier in Spain.

The upper right panel in figure 2 shows a cross sectional drawing of the lower test mass. The test masses were made from oxygen free, high-conductivity (OFHC) copper and were coated with a thin layer of gold to prevent oxidation; no ferromagnetic adhesion layer was used in this coating process. Copper was the material of choice to avoid magnetic forces on the masses. Each test mass was a few grams less than 1100 g. The test masses were 100 g heavier than the nominal 1 kg load of the balance. This was possible, because 100 g was removed from the mass pan of the mass comparator to make it vacuum compatible. The stability of the two gold plated copper masses was acceptable during the course of the experiment. Over the five years of usage, the value of each mass was determined eight times at a calibration laboratory. The mass of each test mass varied by less than 440 μ g or in relative terms less than 4×10^{-7} .

The mass exchanger allows either one of the two test masses to be connected to the balance. Each test mass is suspended by two wires from an aluminum cross bar. The two cross bars are perpendicular to each other and vertically displaced. Each cross bar can either be suspended from a stirrup that is suspended from the mass pan of the balance or to a hydraulic actuated arm. Each arm can be moved vertically by a few millimeters. Lowering the arm places the crossbar onto the stirrup and hence connects the test mass to the balance. The mass exchange algorithm was programmed such that there was always a 1100 g load on the balance. During mass exchange one arm was lowered, while the other was simultaneously raised.

To avoid buoyancy and other gas pressure forces, the vessel containing the balance and a tube surrounding the test masses were evacuated to pressures around 10^{-4} Pa. The upper right panel in figure 2 shows a drawing of the lower test mass, the vacuum tube surrounding it and its position relative to the lower field mass in the apart position.

A view of the experiment described above is given in the left panel of figure 2. The experiment was located in

¹Certain commercial equipment, instruments, or materials are identified in this paper in order to specify the experimental procedure adequately. Such identification is not intended to imply recommendation or endorsement by the National Institute of Standards and Technology, nor is it intended to imply that the materials or equipment identified are necessarily the best available for the purpose

a pit at the Paul Scherrer Institute (PSI) in Villigen, Switzerland. The pit was divided into an upper and a lower room separated by a false floor. The lower room contained the TM's and FM's. The upper room contained a thermally insulated chamber housing the vacuum vessel with the balance. The vacuum vessel rested on a granite plate that sat on two steel girders spanning the pit. This mounting ensured that the balance was decoupled from the field mass assembly which was anchored to the bottom of the pit. The upper room of the pit housed the control electronics, the computers and the vacuum pumps. The temperature inside the thermally insulated chamber surrounding the balance was actively controlled; the temperature was stable within 0.01 K. The air temperature of the lower part of the pit was actively controlled to within ≈ 0.1 K. Thirteen tons of mercury make a great thermometer. A temperature rise of only a few kelvin would have been enough to bring the mercury level to the top rim of the compensation vessel.

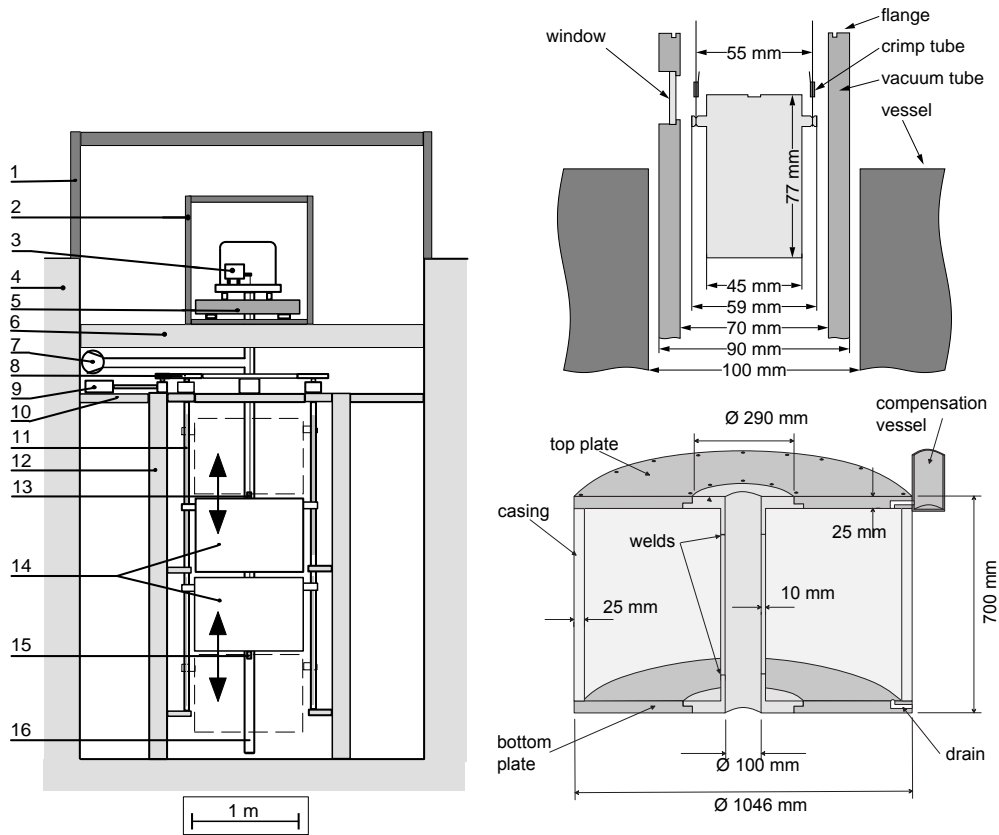


Figure 2: On the left is a side view of the experiment. Legend: 1=measuring room enclosure, 2=thermally insulated chamber, 3=balance, 4=concrete walls of the pit, 5=granite plate, 6=steel girder, 7=vacuum pumps, 8=gear drive, 9=motor, 10=working platform, 11=spindle, 12=steel girder of the main support, 13=upper TM, 14=FM's, 15=lower TM, 16=vacuum tube. On the lower right, a drawing of one of the vessels holding the liquid mercury. On the upper right, a cross-sectional view of the lower test mass in the vacuum tube.

3 Linearity and calibration of the mass comparator

A large amount of time was spent understanding and improving the calibration procedure of the mass comparator that was employed in the first measurement [9] of G made with this apparatus. However, questions remained about the linearity of the balance, i.e., is the calibration of the mass comparator that was performed with a 1 g mass valid at a signal level of $785 \mu\text{g}$ (see top panel of Fig. 3)? Nonlinearity measurements on a laboratory balance (AT261) with a measuring range of 200 g were performed by engineers at Mettler Toledo. By scaling their results to the mass comparator used in the G experiment, an upper limit for a possible bias due to the nonlinearity was estimated to be 200×10^{-6} of the result. In the 1998 result, the nonlinearity of the balance was the largest entry in the uncertainty budget.

Calibrating a balance in the range of 800 μg is not a simple problem. The obvious solution of using a calibration mass of approximately 1 mg does not work for the present G measurement as the uncertainty of such a small mass relative to the international prototype of the kilogram is of the order of 500×10^{-6} , i.e., more than an order of magnitude larger than the desired accuracy of the G measurement. E. Holzschuh suggested the principle that was finally used to solve this problem. The basic idea is the following: The nonlinearity of a balance can be averaged away by measuring the gravitational signal, not just at one point of the transfer function, but at many points equally spaced within a calibration range defined by a calibration mass having a sufficiently accurate absolute mass. A deeper rationale for this method comes from the fundamental theorem of analysis which basically says that the average of the local slopes of a Riemann integrable function is the same as the slope of a line connecting the start and the end points of the averaging interval. The different points of the measurement are easily obtained by adding small masses to the balance pan having roughly equal weights. Their masses need to be known only relative to one another. For the implementation of this calibration method, we employed 256 mass steps of approximately 785 μg over a calibration range of 200 mg.

Although the basic principle of this method is based on equal mass steps over a calibration range, it is difficult to make small masses with exactly equal mass. In addition, it was not always possible to make all mass steps due to malfunction of the auxiliary mass handler. A somewhat more general analysis method was developed to overcome these problems. For this purpose, a series of Legendre polynomials with an arbitrary highest order L_{max} was chosen. Hence, the calibrated reading of the balance $f(u)$ as a function of the mass u on the mass pan can be written as

$$f(u) = \sum_{\ell=0}^{L_{\text{max}}} a_{\ell} P_{\ell}(\xi), \quad (4)$$

where P_{ℓ} is a Legendre polynomial of order ℓ and $\xi = 2u/u_{\text{max}} - 1$. Two constraints, $f(0) = 0$ and $f(C) = C$, reduce the number of degrees of freedom from $L_{\text{max}} + 1$ to $L_{\text{max}} - 1$ where C is the sum of the two calibration masses. Thus, the values of a_0 and a_1 are given by

$$a_0 = C/2 - \sum_{\text{even } \ell=2}^{L_{\text{max}}} a_{\ell} \quad \text{and} \quad a_1 = C/2 - \sum_{\text{odd } \ell=3}^{L_{\text{max}}} a_{\ell}. \quad (5)$$

The remaining $L_{\text{max}} - 1$ parameters a_{ℓ} , and the size of the signal s/g , were obtained by minimizing

$$\chi^2 = \sum_{n=1}^N [f(u_n + s/g) - f(u_n) - y_n]^2 \sigma_n^{-2},$$

where y_n is the calibrated reading obtained with offset u_n and σ_n is the statistical standard deviation of the reading. The minimization of χ^2 is straightforward. Since s/g is the only nonlinear parameter, a one parameter search for a minimum is all that is required. The a_{ℓ} parameters are linear and can be solved by a trivial matrix inversion. The number of parameters required for a reasonable fit can be determined from the value of χ^2 .

The small masses used for shifting the measuring point are referred to as auxiliary masses (AM). Two sets of AMs were employed. One set (AM-1) contained 16 masses with an average value of 783 μg and a standard deviation of 1.5 μg . The other set (AM-2) contained 16 masses with an average mass of 16 times 783 μg and a standard deviation of 2.3 μg . With combinations of these two sets of masses it is possible to have 256 approximately equal mass steps in the calibration interval from 0 to 200 mg. The masses of AM-1 and AM-2 were made from stainless steel wire with a diameter of 0.1 mm and 0.3 mm, respectively.

The device for loading the masses on the balance is shown in the lower left panel of figure 3. Initially, each set of masses rests on one of the two separately controlled double staircases bracketing a narrow metal strip attached to the balance pan. The steps are 2 mm high and 2 mm wide. They are arranged in the form of a “V”. The vertical position of each staircase is controlled by a rack and pinion device driven by a stepper motor. Lowering the staircase places alternately a mass from the right side of the “V” and then one from the left side on the balance pan. This keeps the off-center loading of the balance pan small.

Very little nonlinearity was observed. The value of s/g obtained from the χ^2 minimization above changed from 784.899 4 μg for a linear transfer function, i.e., $L_{\text{max}} = 1$ to a value of 784.900 5 μg for $59 \leq L_{\text{max}} \leq 66$. For the final published result the latter value was used, yielding a value for G that is only 1.4×10^{-6} larger than the value we would have obtained with no correction. The numbers above are a reflection of the good design of the balance

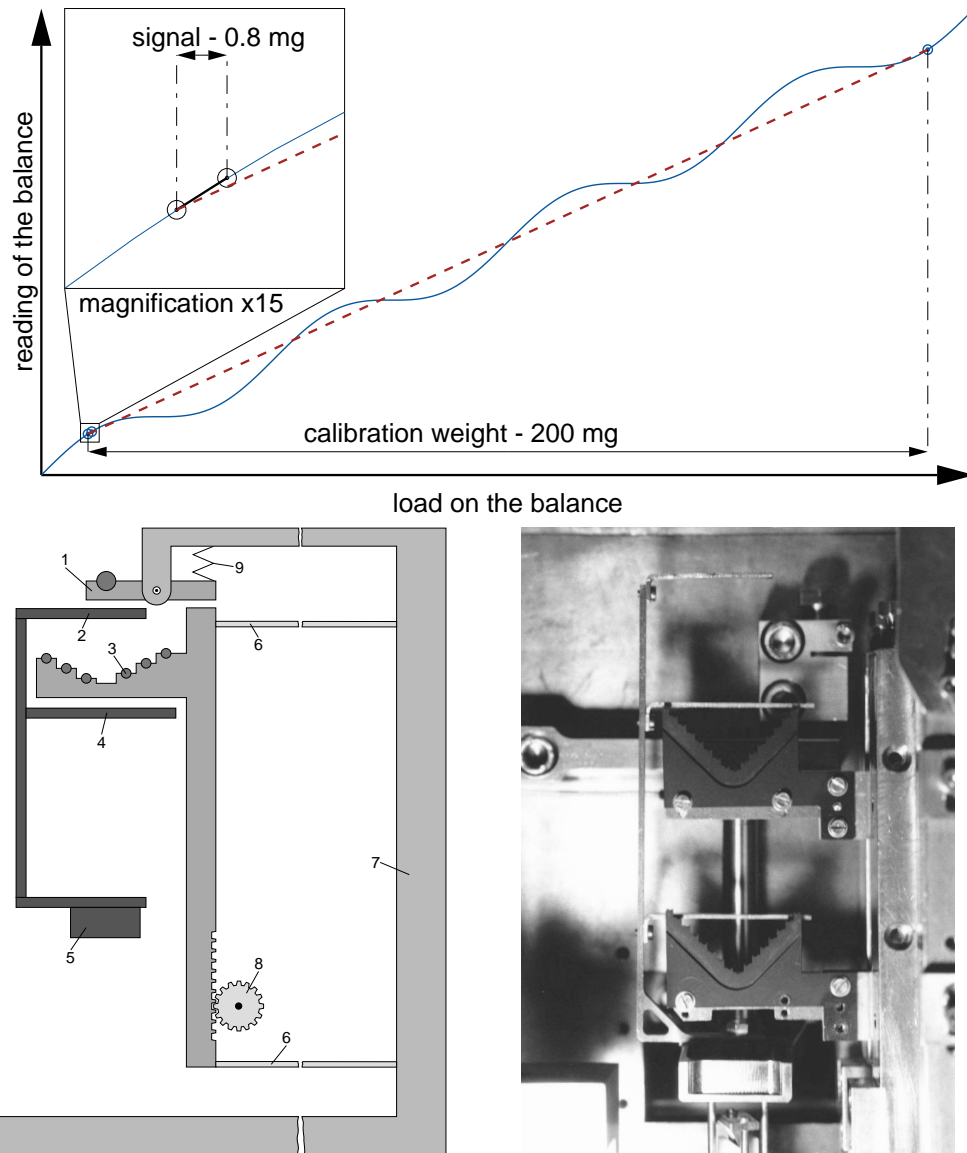


Figure 3: The upper panel schematically illustrates the effect of a nonlinearity in the balance on the measurement. The top graph shows the transfer function of the balance, i.e. reading on the vertical axis as a function of load on the horizontal axis. Since the calibration weight is over 250 times larger than the signal it is not clear that the slope of transfer function at the working point is identical to that of the calibration. The figure in the lower left panel is a schematic drawing of the mass handler with the following legend: 1=pivoted lever pair holding a CM, 2=narrow strip to receive the CM, 3=double stair case pair holding AM's, 4=narrow strip to receive AM's, 5=balance pan, 6=flexure strip, 7=frame, 8=rack and pinion, and 9=coil spring. The lower right panel shows a photograph of the mass handler during installation.

and provide increased confidence in the measurement result, since the value of G is independent of the subtleties of the data analysis. In the end, it was worth tracking down this problem and putting the specter of nonlinearity in this experiment to rest, once and for all.

The mass handler also doubles as a device to place either of two calibration masses (CMs) on the balance pan. Each rested on a spring-loaded double lever. By raising each staircase, one of the CMs is placed on the balance pan. Each calibration mass had a nominal value of 100 mg and was made from stainless steel wire.

The CMs were calibrated at the Swiss Federal Institute of Metrology (METAS) before and after each measurement campaign. In total, three measurement campaigns were performed. Unfortunately in the last two campaigns problems with the mass handler rendered the data unsuitable for a G determination. Hence, only data from the

first campaign were used to determine the final value of G .

Water adsorption on the calibration masses is a concern. The three calibrations made by METAS were performed in air, i.e., with an ubiquitous water film on the steel wires. In the experiment, however, the weight in vacuum was important. To experimentally investigate this effect, wires with two different diameters, 0.96 mm and 0.5 mm, were used to make the CMs. Hence, the surface area of the CM with the thinner wire was almost twice that of the thicker wire. It was found that the weight difference of the two CMs in vacuum was consistent with their difference measured by METAS in air. Hence, no sorption effect could be detected. We placed an upper limit on the sorption effect using sorption coefficients from the literature [15]. Since the vacuum environments are difficult to compare, a generous relative standard uncertainty of 100% was assigned to these values.

Having two calibration masses made the calibration process more robust. The mass difference between the CMs determined in the first and second calibrations made by METAS changed by $1.0 \pm 0.5 \mu\text{g}$, i.e., $5 \pm 2.5 \times 10^{-6}$ of their combined weight. Their weight difference in vacuum was found to be consistent with the first METAS calibration. Since in the second and third measurements in vacuum, the CM weight difference was consistent with the second and third METAS calibration, only one viable hypothesis could explain these observations: One wire lost a small dust particle or even a part of the wire itself during transfer from the measurement at PSI to the calibration measurement at METAS. Note that the wire that lost the particle was the thicker wire that had jagged edges from being cut by a wire cutter. Based on this hypothesis we used the values obtained by METAS during the first calibration to analyze our data.

From these measurements, we are confident that our result for G is based on an SI traceable calibration of the measured gravitational signal. In the end, a relative standard uncertainty of 7.3×10^{-6} was assigned to calibration and nonlinearity. We acknowledge that the observed mass change of $1 \mu\text{g}$ in one of the calibration masses was not desirable. However, after careful review of the mass differences obtained in air and in vacuum we have found the only possible explanation. The nonlinearity of the balance has a small effect on the result and was certainly not as large as the conservative uncertainty given in 1998.

4 Measurements and Result

The data used in the final G result were measured during 44 days in the late summer of 2001. Figure 4 shows the measured weight difference between the two test masses for the two field-mass positions. One can see a balance drift and other disturbances, e.g., a jump on day 222 most likely caused by loss or gain of a dust particle. However, all these effects are common mode, i.e., they cancel in the second difference.

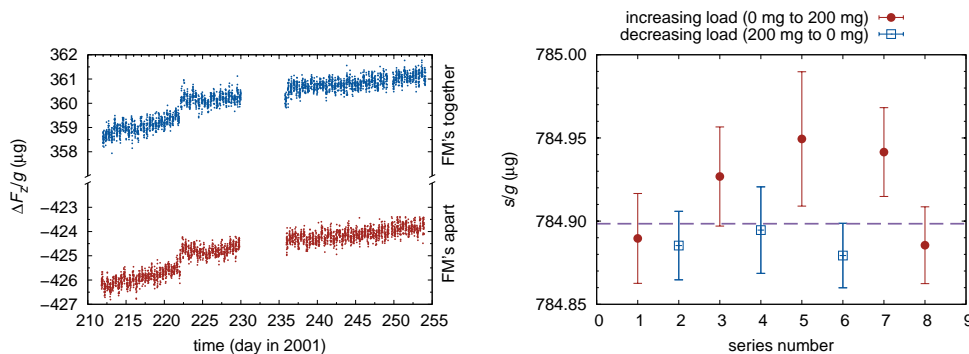


Figure 4: On the left, the measured weight difference in μg between TM's for the FM's positions apart and together. Note the break in the vertical axis. On the right, the average signal for each of the eight cycles. Cycles with increasing load are shown as circles. Cycles with decreasing load are shown as squares. The dashed line is the average of all eight series. The error bars give the type A uncertainties of the weighings.

The data shown in figure 4 consists of eight nearly complete cycles. A cycle is a measurement of G with all 256 possible load values that can be achieved with the two sets of auxiliary masses, two test masses and the apart and together positions of the field masses. There are 2304 individual weighings in one complete cycle. The load was either applied in an increasing (from 0 mg to 200 mg) or decreasing (from 200 mg to 0 mg) fashion. Of the

Table 1: Relative type A and type B uncertainties of G as determined in this experiment. All numbers are relative standard uncertainties ($k = 1$).

Description	Type A (10^{-6})	Type B (10^{-6})
Weighings	11.6	
TM-sorption	7.4	7.4
Linearity	6.1	
Calibration	4.0	0.5
Mass Integration	5.0	3.3
Total	16.3	8.1

eight cycles, five were taken in increasing order. The measured value of the gravitational signal is shown on the right panel of figure 4.

The uncertainty budget is shown in table 1. The largest contribution is from the statistical scatter of the weighing data contributing a relative uncertainty of 11.6×10^{-6} . The next largest effect is water sorption on the test masses. Combining type A and type B uncertainties in this category yields a relative uncertainty of 10.5×10^{-6} . This effect is due to a different air flow around the vacuum tube for the FMs in position A and T. Hence, the temperature of the vacuum tube changes slightly; about 0.04 K and 0.01 K for the regions around the upper and lower test mass respectively. This temperature change will result in a redistribution of the adsorbed water layers on the vacuum tube and the test masses. Changing the water layer on the test masses coherently with the field mass position will introduce a bias into the gravitational signal.

The effect of the temperature change was measured in a dummy experiment. The FM's were not moved, but the vacuum tube surrounding the test masses was heated while the weight variation was recorded. The heating of the vacuum tube produced a temperature variation about 10 times that observed in the G experiment. Scaling the result of the dummy measurement to the experimental conditions yielded the result that the measured signal of $784.8994 \mu\text{g}$ needed to be corrected by $-0.0168(82) \mu\text{g}$. This correction resulted in a type A relative standard uncertainty of 7.4×10^{-6} . An additional 7.4×10^{-6} was assigned as a type B relative uncertainty to reflect the uncertainty in scaling the temperature conditions to those of the actual G measurement. This result supersedes the 49×10^{-6} relative uncertainty listed in the 1998 experiment. That value was an estimate based on a measurement in which the temperature change of the vacuum tube near the upper test mass was approximately 200 times the amplitude of the temperature variation in the G experiment.

The final result of the Zürich G experiment is

$$G = 6.674\,252(122) \times 10^{-11} \text{ m}^3 \text{ kg}^{-1} \text{ s}^{-2}. \quad (6)$$

Figure 5 shows this result in relationship to other results. It is noteworthy that the Zürich G experiment is only one of four experiments that do not use torsion balances. Of the three other experiments, two employed simple pendula and one experiment used an atom interferometer. Out of these four experiments only two, the Zürich experiment and the experiment by Parks and Faller [19] have reached a relative standard uncertainty below 10^{-4} .

5 Discussion of the experiment

Almost a decade has past since the final report of the Zürich G experiment was published. In this decade, our experience and views evolved and in hindsight we would like to give an honest assessment of certain features of the experiment. From this vantage point, different aspects seem more important than in the past when all of us were immersed in performing or analyzing the experiment.

5.1 Calibration

The strongest point of the experiment is that it has a traceable and credible calibration. In section 3 most details on the calibration of the balance are given. The calibration was performed in situ. Furthermore, unlike

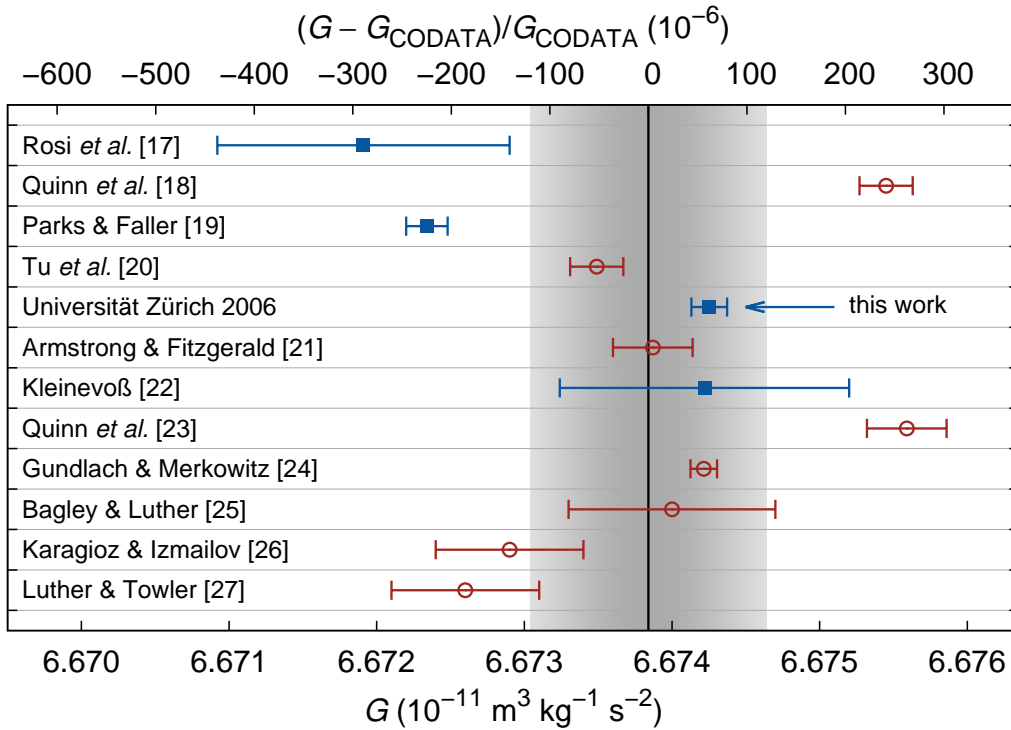


Figure 5: The result of the Zürich G experiment in relation to the results of other experiments. The experiments denoted by open circles were using torsion balances to measure G . The four data points denoted solid squares were obtained by different methods. One measurement was performed using an atom interferometer, two measurements with a pair of pendula, and ours utilized a beam balance. The shaded area in the center of the graph denotes the $1 - \sigma$ confidence interval of the CODATA adjusted value from the 2010 adjustment [16]. The years indicate when the results were published. The values and uncertainties can be found in the references [17, 18, 19, 20, 21, 22, 23, 24, 25, 26, 27].

in most torsion balance experiments, the calibration was performed in the same mode, i.e., the configuration of the experiment remained the same. Another interesting aspect of this experiment is the fact that the calibration takes advantage of gravitation itself. The gravitational force between a known mass and the earth was used. This is in contrast to torsion balances, which are often calibrated using electrostatic forces.

5.2 Nonlinearity

In 1995 Kuroda pointed out [28] a nonlinear effect in torsion balances that could lead to a significant systematic bias in the so-called time of swing method. This nonlinearity arises from anelasticity [29] in the torsion fiber, i.e., the torsional spring constant is a function of frequency and can add a relative systematic bias up to 10^{-4} to these experiments. With Kuroda's publication nonlinearity became a prime concern in experiments determining the gravitational constant. Unfortunately, most of the effort is spent on anelasticity of torsion fiber. This is certainly an important, but not the only source, of nonlinearity.

Nonlinearity can occur in any instrument. Linearity of an experimental apparatus should never be taken for granted. After obtaining a first result with the Zürich G experiment in 1998, the experimenters were unable to ascertain the linearity of the mass comparator and a generous relative uncertainty of 200×10^{-6} was assigned to it.

Subsequently the nonlinearity was investigated, see section 3. The result showed a remarkably small contribution due to nonlinearity of the mass comparator. The relative standard uncertainty due to nonlinearity was only 6.1×10^{-6} . Although the nonlinearity of the balance was not a large effect in our experiment, it was a good investment of time and effort to know this for certain.

5.3 Large gravitational signal

The gravitational signal in this experiment is large, i.e., the second difference corresponds to $7.7 \mu\text{N}$. For comparison with the torsion-pendulum measurements of [18] and [24], the corresponding gravitational forces are approximately $0.3 \mu\text{N}$ and $1.5 \times 10^{-4} \mu\text{N}$, respectively. Thus, the force producing the signals in these two measurements are a factor of 25 and 50,000 times smaller than that of the Zürich experiment.

Having a large gravitational force acting on the test masses reduces the relative size of parasitic forces that arise due to surface potentials, gas pressure forces, and other disturbances.

5.4 Symmetry and geometry

The experiment has beautiful symmetry. This symmetry is one of the key points enabling the precision that the experiment finally achieved. The center of mass of the field masses remains at one point. The field masses are supported by three spindles that have a right-hand thread on the upper part and a left-hand thread on the lower part. Thus, as one field mass moves down it pushes the other field mass up. Other than friction, no mechanical work is performed in moving from position A to position T. Therefore, a relatively small motor was used to move the field masses. As an example, to overcome the potential energy of raising one field mass in the five minutes that it takes to change from position A to T, 180 W of power would be required.

Besides motor power vs. temperature, the symmetric setup has another advantage: The system does not tilt. The support structure that connects the field-mass assembly to the ground of the experiment has to take up the same force and torques independent of the field mass position.

The gravitational field on axis of a hollow cylinder centered at the origin with inner diameter R_1 , outer diameter R_2 , height $2B$, and density ρ is given by

$$V^{(1)} = g_z(0, 0, z) = 2\pi\rho G \left(r_2^+ - r_2^- + r_1^- - r_1^+ \right) \text{ with } r_{1,2}^\pm = \sqrt{R_{1,2}^2 + (z \pm B)^2}. \quad (7)$$

The potential off axis can be found easily by using a Taylor expansion of $g_z(r, 0, z)$ for small r . Assuming azimuthal symmetry will yield non-zero coefficients only for even exponents of r .

From the above equation, it can be seen that the vertical component of the gravitational field near the end of the hollow cylinder ($r = 0, z \approx B$) has the shape of a saddle surface, i.e., it has a maximum along the axial direction and a minimum in the radial direction. Since the test masses are located at the saddle points, the accuracy required to measure their position can be achieved with only moderate effort. The vertical and horizontal positions of both test masses relative to the field masses were obtained with an accuracy of about 0.1 mm in the horizontal direction and 0.035 mm in the vertical direction. The measurements were performed using surveyors' tools: a theodolite for horizontal positions and a leveling instrument for vertical positions.

While we only had to measure the positions of the test masses with moderate precision, the mass distribution of the inner parts of the vessels had to be known with high accuracy. Hence, these parts were machined with tight tolerances and measured on a coordinate measuring machine with small uncertainties. For example, the central bores of the hollow cylinders were honed to achieve the required standard uncertainty of $1 \mu\text{m}$ on the inner diameter.

The uncertainties of the dimensions of the test masses, of the dimensions of the field masses, and of their relative positions sum up to relative standard uncertainty in the final result of 4.95×10^{-6} . This number includes the mercury density and mass via the constraint fit, see 5.6. This uncertainty is part of the 5.0×10^{-6} listed under Type A and mass integration. The remainder is due to uncertainties in the mass measurements of the steel components of the vessels.

5.5 Vertical system

From an objective viewpoint, measuring along the direction of local gravity is a terrible thing to do. One has to measure the minuscule gravitational signal ($785 \mu\text{g}$) on top of a large background (1 kg). The ratio of background to signal is 1.3×10^6 . Since the sensitivity of the experiment is 10^{-5} times the signal, the ratio of sensitivity to background is 1.3×10^{11} . This is a really large ratio for a mechanical experiment. From these numbers it is obvious that a vertical experiment needs a much higher ratio of sensitivity to background than a horizontal experiment. This is one of the reasons why several attempts in this geometry achieved uncertainties of 10^{-3} or larger [30, 31].

Two factors mediate this disadvantage in the Zürich G experiment: First, the mass comparator is constructed such that a large fraction of the applied force is balanced by a built in counter mass and only a small part of the force (4×10^{-3}) has to be produced by an electromagnetic actuator. Second, state of the art mass comparators have a fantastic sensitivity. The commercial version of the AT1006 has a relative resolution of 10^{-10} .

5.6 Liquid field masses

The experiment employs two liquid field masses, i.e., 90% of the gravitational signal is contributed by liquid mercury and only about 10% by both vessels. A liquid minimizes density inhomogeneities at the expense of requiring a vessel that can hold the liquid. Indeed, the uncertainty in the density inhomogeneity of the mercury was only a small contribution to the total uncertainty of the experiment. The absolute value of the density of mercury was determined at the Physikalisch Technischen Bundesanstalt (PTB) in Germany with a relative uncertainty of 3×10^{-6} . From this measurement, the known temperature, thermal expansion and isothermal compressibility a density profile of the mercury in the vessels could be calculated. Modeling the vessels for the mass integration was cumbersome. Both vessels were broken up in 1200 objects, with positive and negative density. Simple rotational shapes with rectangular, triangular or circular cross sections were used. Negative density was employed to take away from previously modeled space. This was used, e.g., for bolt holes, and O-ring grooves.

While mercury had a known density gradient due to its compressibility, density variations in the stainless steel used to manufacture the vessels were unknown. This was especially problematic for the parts that were close to the test masses. A density variation in these parts could have affected the result of the experiment. In order to investigate this, the inner pieces of the vessels were cut into rings after the experiment ended (three rings near the top and three near the bottom of each central tube). The density of each ring was determined by weighing each ring and measuring its dimensions with a coordinate measuring machine. With this method, a standard uncertainty of 0.001 g cm^{-3} was achieved. The average density of the rings was 7.908 g cm^{-3} . The largest variation of the density was only 0.1%, which had only a negligible effect on the mass-integration constant.

Another interesting issue arose from deformation after loading the vessels with mercury. The four main parts used to assemble each vessel were carefully measured on a coordinate measuring machine (CMM). However, the load and hydrostatic pressure deformed the vessels. To take this into account, the shape of the top and bottom of the full vessels were measured with a laser tracker (LT). From the CMM and LT measurements combined with equations describing the bending of thin cylindrical shells [32] the final shape of the vessels could be determined.

The liquid field masses had one, originally not anticipated, advantage: Since the geometrical dimensions of one mercury volume (inner radius r , outer radius R , height h), the mass of the mercury m , and the density of the mercury was known, one could set up a system of equations with a constraint on the volume, mass and density. By using a least squares adjustment of χ^2 given by

$$\chi^2 = \left(\frac{r - r_0}{\sigma_r}\right)^2 + \left(\frac{R - R_0}{\sigma_R}\right)^2 + \left(\frac{h - h_0}{\sigma_h}\right)^2 + \left(\frac{m - m_0}{\sigma_m}\right)^2 + \left(\frac{\rho - \rho_0}{\sigma_\rho}\right)^2 \quad (8)$$

the uncertainties on the four parameters can be substantially improved. Here, the quantities with subscript denote measured values or their standard uncertainties and those without subscript refer to the adjusted values. This procedure introduces correlations between the adjusted parameters, but this is a small price to pay compared to the improvement in uncertainty: By using the constraint the uncertainty component caused by the geometric uncertainties in the mass integration could be reduced by a factor of 7.

6 Summary

From 1994 to 2006 seven scientists worked on the Zürich G experiment with various degrees of overlap. Their combined work resulted in the value $G = 6.674\,252(122) \times 10^{-11} \text{ m}^3 \text{ kg}^{-1} \text{ s}^{-2}$. The relative standard uncertainty of the measurement is 18×10^{-6} . In recent history this experiment is only one of two experiments that have not used a torsion balance and have produced a result with a relative uncertainty smaller than 100×10^{-6} .

Torsion balances are very sensitive instruments and are well adapted to the measurement of small forces such as gravitational forces. However, calibrating a torsion balance is difficult and error-prone [33]. Furthermore, nonlinearities can be a significant effect in measurements using torsion balances [28]. Although the calibration of

a beam balance is simple and robust, the gravitational signal has to be measured in the presence of a very large background due to the weight of the test mass. However, as we have demonstrated, it is possible to obtain a relative statistical accuracy of several parts in 10^6 with this method.

Considering the differences and difficulties of the various approaches, only more data will finally help to resolve the debate concerning the true value of G . We hope to see many different experimental approaches in the future and we encourage the researchers to invest in a credible and traceable calibration scheme.

References

- [1] Fischbach E, Sudarksy D, Szafer A, Talmadge C, Aronson SH. 1986 Reanalysis of the Eötvös Experiment. *Phys. Rev. Lett.* **56**, 3-6.
- [2] v. Eötvös R, Pekár D, Fekete E. 1922 Beiträge zum Gesetze der Proportionalität von Trägheit und Gravität. *Ann. Phys.* **68**, 11-66.
- [3] Stubbs CW, Adelberger EG, Raab FJ, Gundlach JH, Heckel BR, McMurry KD, Swanson HE, Watanabe R. 1987 Search for an intermediate-range interaction. *Phys. Rev. Lett.* **58**, 1070-1073.
- [4] Cornaz A, Hubler B, Kündig W. 1994 Determination of the gravitational constant at an effective interaction distance of 112 m. *Phys. Rev. Lett.* **72**, 1152-1155.
- [5] Hubler B, Cornaz A, Kündig W. 1995 Determination of the gravitational constant with a lake experiment: New constraints for non-Newtonian gravity. *Phys. Rev. D* **51**, 4005-4016.
- [6] Schlamminger St, Holzschuh E, Kündig W, Nolting F, Pixley RE, Schurr J, Straumann U. 2006, Measurement of Newton's gravitational constant. *Phys. Rev. D* **74**, 082001 1-25.
- [7] Nolting F. 1998 Determination of the gravitational constant by means of a beam balance: design, construction and first results. Ph.D. Thesis, University of Zürich, Zürich, Switzerland.
- [8] Schlamminger S. 2002 Determination of the gravitational constant using a beam balance. Ph.D. Thesis, University of Zürich, Zürich, Switzerland.
- [9] Schurr J, Nolting F, Kündig W. 1998 Gravitational constant measured by means of a beam balance. *Phys. Rev. Lett.* **80**, 1142-1145.
- [10] Schurr J, Nolting F, Kündig W. 1998 Measurement of the gravitational constant G by means of a beam balance. *Phys. Lett. A* **248**, 295-308.
- [11] Nolting F, Schurr J, Kündig W. 1999 Determination of G by means of a beam balance. *IEEE Trans. Instrum. Meas.* **48**, 245-248.
- [12] Nolting F, Schurr J, Schlamminger St, Kündig W. 1999 A value for G from beam-balance experiments. *Meas. Sci. Technol.* **10**, 487-491.
- [13] Nolting F, Schurr J, Schlamminger St, Kündig W. 2000 Determination of the gravitational constant G by means of a beam balance. *EuroPhysics News* **31**, 25-27.
- [14] Schlamminger St, Holzschuh E, Kündig W. 2002 Determination of the gravitational constant with a beam balance *Phys. Rev. Lett.* **89**, 161102 1-4.
- [15] Schwartz R. 1994 Precision determination of adsorption layers on stainless steel mass standards by mass comparison and ellipsometry Part 2: sorption phenomena in vacuum *Metrologia* **31** 129-136.
- [16] Mohr PJ, Taylor BN, Newell DB. 2012 CODATA recommended values of the fundamental physical constants: 2010 *Rev. Mod. Phys.* **84**, 1527-1605.
- [17] Rosi G, Sorrentino F, Cacciapuoti L, Prevedelli M, Tino GM. 2014 Precision measurement of the Newtonian gravitational constant using cold atoms *Nature* **510** 518-521.

- [18] Quinn T, Parks H, Speake C, Davis R. 2013 Improved determination of G using two methods. *Phys. Rev. Lett.* **111**, 101102 1-5.
- [19] Parks HV, Faller JE. 2010 Simple pendulum determination of the gravitational constant. *Phys. Rev. Lett.* **105**, 110801 1-4 (2010).
- [20] Tu L-C, Li Q, Wang Q-L, Shao C-G, Yang S-Q, Liu L-X, Liu Q, Luo J. 2010 New determination of the gravitational constant G with time-of-swing method. *Phys. Rev. D* **82** 022001 1-36.
- [21] Armstrong TR and Fitzgerald MP. 2003 New measurements of G using the measurement standards laboratory torsion balance *Phys. Rev. Lett.* **91** 201101 1-4.
- [22] Kleinevoß U 2002 Bestimmung der Newtonschen Gravitationskonstanten G . Ph.D. Thesis, University of Wuppertal, Wuppertal, Germany.
- [23] Quinn TJ, Speake CC, Richman SJ, Davis RS, Picard A. 2001 A new determination of G using two methods. *Phys. Rev. Lett.* **87**, 111101 1-4 (2001).
- [24] Gundlach JH, Merkowitz SM. 2000 Measurement of Newton's constant using a torsion balance with angular acceleration feedback. *Phys. Rev. Lett.* **85**, 2869-2872.
- [25] Bagley CH, Luther GG. 1997 Preliminary results of a determination of the Newtonian constant of gravitation: a test of the Kuroda hypothesis. *Phys. Rev. Lett.* **78**, 3047-3050.
- [26] Karagioz OV, Izmailov VP. 1996 Measurement of the gravitational constant with a torsion balance. *Measurement Techniques* **39**, 979-987.
- [27] Luther GG, Towler WR. 1982 Redetermination of the Newtonian Gravitational Constant G *Phys. Rev. Lett.* **48**, 121-123.
- [28] Kuroda K. 1995 Does the time-of-swing method give a correct value of the Newtonian gravitational constant? *Phys. Rev. Lett.* **75** 2796-2798.
- [29] Speake CC, Quinn TJ, Davis RS, Richman SJ. 1999 Experiment and theory in anelasticity. *Meas. Sci. Technol.* **10** 430-434.
- [30] Schwarz JP, Robertson DS, Niebauer TM, Faller JE. 1999 A new determination of the Newtonian constant of gravity using the free fall method. *Meas. Sci. Technol.* **10**, 478-486.
- [31] Lamporesi G, Bertoldi A, Cacciapuoti L, Prevedelli M, Tino GM. 2008 Determination of the Newtonian Gravitational Constant Using Atom Interferometry. *Phys. Rev. Lett.* **100**, 050801 1-4 (2008).
- [32] Timoshenko SP, Woinowsky-Krieger S, Theory of Plates and Shells, McGraw-Hill, New York(1987).
- [33] Michaelis W, Melcher J, Haars H. 2004 Supplementary investigations to PTB's evaluation of G . *Metrologia* **41** L29-L32.